A Reflected-Wave Ruby Maser with *K*-Band Tuning Range and Large Instantaneous Bandwidth

CRAIG R. MOORE, MEMBER, IEEE, AND ROBERT C. CLAUSS, ASSOCIATE MEMBER, IEEE

Abstract—**A novel maser concept is outlined and a unique design described which permits wide bandwidth and waveguide tuning range by employing four stages cascaded via cryogenically cooled circulators. Theoretical considerations for gain, bandwidth, gain ripple, and noise temperature are included. Operated on a closed-cycle helium refrigerator with a superconducting persistence-mode magnet, the four-stage amplifier is tunable from 18.3 to 26.6 GHz with 30 dB of net gain and achieves 240 MHz of 3-dB bandwidth near the center of this band. The measured noise temperature is 13±2 K referred to the room-temperature input flange. Applications are foreseen utilizing cooled parametric downconverters and upconverters with this amplifier at IF to extend the low-noise performance up to millimeter frequencies and down to *L*-band for radio astronomy and planetary spacecraft communication.**

I. Introduction

MASERS are well known as the lowest noise microwave amplifiers. However, because of the need to operate at liquid-helium temperatures, and the moderate bandwidths available (usually <60 MHz), nonlaboratory applications have been generally limited to spectral-line radio astronomy, radar astronomy, and spacecraft communications [1]–[4]. Masers with large instantaneous bandwidth (200 to 500 MHz) and waveguide band tuning range would find application in continuum radio astronomy, and as IF amplifiers for millimeter wavelength receivers employing cooled mixers. In these applications, the increased bandwidth is necessary to many scientific experiments, and the wide tuning range provides versatility, easing the design of millimeter mixers. By combining a wide-band maser with cooled parametric upconverters and downconverters, a band-switched receiver can be realized which would facilitate very-wide-frequency coverage in the present lowest noise applications [5].

The maser development described here was a cooperative effort between the National Radio Astronomy Observatory (NRAO) and the Jet Propulsion Laboratory (JPL), under a contract from NRAO. This represents a continuation of activity in maser development at JPL for the National Aeronautics and Space Administration since 1958 and an interest in furthering the state of the art in low-noise receivers on the part of NRAO.

Manuscript received May 18, 1978; revised October 20, 1978. This paper presents work which was made possible through prior maser research carried out at the Jet Propulsion Laboratory, California Institute of Technology, under Contract NAS 7-100 sponsored by the National Aeronautics and Space Administration.

C. R. Moore is with the National Radio Astronomy Observatory, Green Bank, WV 24944.

R. C. Clauss is with the Jet Propulsion Laboratory, California Institute of Technology, Pasadena, CA 91103.

II. Description

The reflected-wave maser concept differs from the well-known traveling-wave maser design in the following ways:

1) Circulators are used to direct signals to be amplified to, and from, a slow-wave structure that does not contain resonance isolators. The maser described here uses slow-wave structures consisting of ruby-filled waveguide.

2) The signal being amplified traverses each slow-wave structure twice, once traveling away from and the second time traveling towards the circulator junction.

3) The absence of resonance isolators reduces the slow-wave structure loss [6] and eliminates distortion of the magnetic field required by the maser material. Increased net gain is achieved, and a uniformly low noise temperature (±0.5 K) results across a wide bandwidth when the high gain is traded for bandwidth.

The reflected-wave maser concept differs from the reflection-type cavity maser by using a slow-wave structure instead of a cavity. The reflected-wave maser produces a large gain–bandwidth product, tunable across a wide frequency range. Cavity masers achieve a much smaller gain–bandwidth product at a fixed frequency.

Initial development work on the reflected-wave maser concept began in 1972 under a California Institute of Technology President's Grant[1] to the University of California at San Diego and the Jet Propulsion Laboratory. A successful two stage *X*-band amplifier was built for a laboratory application [7].

The reflected-wave maser described here employs a unique design wherein four stages are cascaded via 10 circulator junctions operating at 4.6 K. The four rubies are biased by a single superconducting magnet, and the 10 circulators are biased in pairs by five sets of permanent

[1]The California Institute of Technology President's Grants are cosponsored equally by the National Aeronautics and Space Administration and California Institute of Technology.

0018-9480/79/0300-0249$00.75 ©1979 IEEE

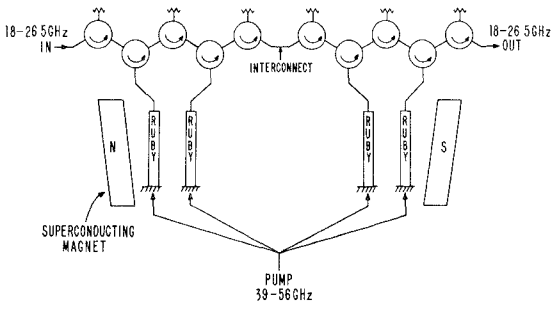

Fig. 1. Schematic diagram of the four-stage K-band ruby maser.

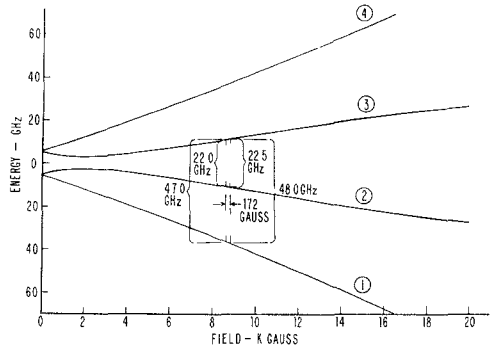

Fig. 2. Energy levels of Cr^{3+} in Al_2O_3 (ruby) at C-axis orientation of 54.733°.

magnets. Each stage has approximately 10 dB of electronic gain and 9.5 dB of net gain, excluding circulator losses. The resulting amplifier (including circulator losses) has a tuning range of 18.3 to 26.6 GHz, at least 30 dB of net gain, up to 240 MHz of 3-dB bandwidth, and a noise temperature of 13 ± 2 K. Further, the design has demonstrated a 400-MHz bandwidth capability.

Fig. 1 depicts the various techniques employed to achieve the wide bandwidth and tuning range. The maser microwave structure consists of a ruby-filled waveguide. Amplification occurs as the signal travels down and back through the ruby. A microwave circulator is used to separate the incoming and outgoing signals. The tuning range is thus limited only by the bandwidth of the circulator. The pump power is injected at the shorted end of the ruby-filled guide, where the pump guide appears as a waveguide beyond cutoff to signal frequencies. The magnetic field biasing the ruby is tapered linearly along the ruby length, giving rise to maser material linewidth spreading. Achieving gain over this broadened linewidth is accomplished by distributing the pump energy in frequency. Frequency modulation is used at a rate with a period much shorter than the pump transition spin relaxation time.

The choice of pink ruby (0.05 percent Cr^{3+} in Al_2O_3) as the active material is based upon years of experience and success with this material at JPL [1], [2]. The selection of optimum-quality material is a vital step in the construction of a multistage maser. Czochralski-grown ruby presently available is free of C-axis wander, misorientation or dislocations, and nonuniform chromium distribution over lengths in excess of 20 cm [8]. With proper annealing, the boule is also quite free of stresses which can cause warpage upon slicing and trimming to size.

Energy levels and transition matrix element values for pink ruby have been tabulated by Berwin [9]; the sensitivity of the transition probabilities to C-axis orientation and the effect of the magnetic biasing field on the transition frequencies are available in detail from this work. These tabulations indicate that the double-pump angle (C-axis orientation 54.7°) is appropriate for operation above 17 GHz. The applicable energy level diagram is shown in Fig. 2, along with the various requirements for wide-band operation. As is implied by the double-pump orientation, the four ground-state energy levels bear a symmetrical relationship. The 1–3 and 2–4 transitions can be pumped simultaneously, as they occur at the same frequency. This results in inversion of the 2–3 transition, which corresponds to the signal frequency. For operation at K-band, the pump frequency is approximately twice the signal frequency plus 3 GHz. For wide-bandwidth operation, the pump frequency must be distributed over a range that is twice the broadened signal frequency resonance separation. The 2–3 transition frequency varies with magnetic field at a rate of approximately 2.9 MHz/G.

III. Maser Gain and Bandwidth

The gain of each stage must be kept below the circulator isolation to insure stability and control feedback-induced ripple. Mismatch at the circulator maser port will cause gain ripple which is highly dependent on gain, as we will show later. At least 30 dB of net gain is desired in order to reduce the noise contribution of the mixer receiver following the maser amplifier. Thus four stages with an electronic gain of 10 dB per stage were selected to achieve the desired performance.

The gain of a linear stagger-tuned maser (linearly tapered magnetic biasing field) is given theoretically as a function of frequency by Siegman [10] as

$$G_{\mathrm{dB}}(f) = \frac{27SN}{Q_m} \frac{\Delta f_L}{2\Delta f_0} \tan^{-1}\left[\frac{(2\Delta f_0/\Delta f_L)}{[2(f-f_0)/\Delta f_L]^2 - (\Delta f_0/\Delta f_L)^2 + 1}\right] \tag{1}$$

where

S slowing factor (c/v_g) (v_g is the group velocity);
N $= l/\lambda_0$, active length of the material in free space wavelengths (l is twice the physical length for a reflected-wave maser);
Q_m magnetic Q;
Δf_L magnetic resonance linewidth of material, MHz;
Δf_0 separation of maser material resonant frequencies due to magnetic biasing field taper, MHz;
f_0 unbroadened resonance frequency (center frequency of instantaneous bandwidth), MHz.

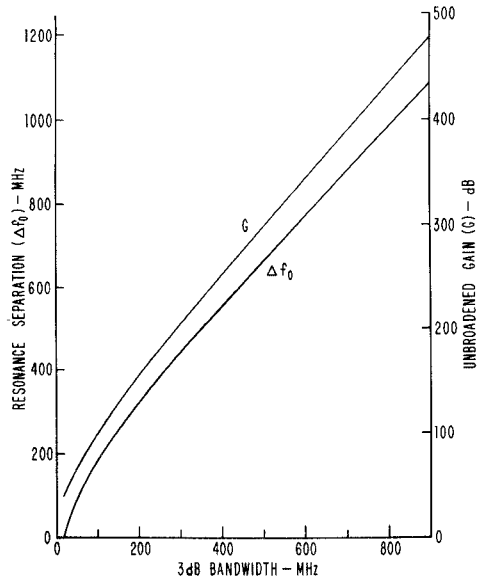

Fig. 3. Unbroadened gain (G) and resonance separation (Δf_0) required to achieve a specified 3-dB bandwidth at 40-dB electronic gain for a linear stagger-tuned ruby maser.

The gain of an unbroadened maser (uniform magnetic biasing field) is given by [10]

$$G_{\text{dB}} = \frac{27SN}{Q_m}. \tag{2}$$

The relationship between unbroadened gain, Δf_0, and the 3-dB bandwidth for a 40-dB gain ruby maser as given by (1) is plotted in Fig. 3. For a 3-dB bandwidth of 250 MHz a Δf_0 of 383 MHz is required; which when combined with a field sensitivity of 2.9 MHz/G requires a linear magnetic field taper of 132 G. Also from Fig. 3, an electronic gain of 40 dB at 250-MHz bandwidth requires an unbroadened gain of 180 dB, or 45 dB per stage. The length of ruby required per stage can be estimated from (2) and the expression for Q_m [10]

$$\frac{1}{Q_m} \approx 10^{-18} \frac{hf}{kT_0} \frac{\mathcal{N}}{n} \frac{IM^2F}{\Delta f_L} \tag{3}$$

where

- h Planck's constant;
- f frequency, Hz;
- k Boltzmann's constant;
- T_0 cryogenic temperature of the maser material, K;
- $\mathcal{N}$ spin density, spins/cm^3;
- n number of energy levels;
- I inversion ratio;
- M maximum value of the transition probability;
- F fill factor;
- Δf_L magnetic resonance linewidth of material, MHz.

The magnetic $Q(Q_m)$ is largely dependent on the maser material, and once the doping and C-axis orientation are optimized only the cryogenic temperature and fill factor are under control of the microwave designer. Since the amplifier is intended to operate on a closed-cycle refrigerator, $T_0 = 4.6$ K. The fill factor is $\frac{1}{2}$, even though the entire waveguide is filled with active material, because the RF magnetic field of the TE_{10} mode signal frequency is linearly polarized and not circularly polarized as it should be for maximum transition probability. The inversion ratio of pink ruby at 22 GHz, 4.6 K, and 54.7° orientation was measured to be 1.8. Under the same conditions, the transition probability M is 1.92, the linewidth Δf_L is 60 MHz, and the spin density $\mathcal{N}$ is approximately 10^{19} cm^{-3}. The magnetic Q is then approximately 30.

The slowing factor includes the effect of the dielectric constant of the ruby but also includes the dispersive characteristic of the waveguide mode. The slowing factor for the TE_{10} mode in a dielectric filled waveguide can be shown to be

$$S = \epsilon \frac{\lambda_{g_\epsilon}}{\lambda_0} = \epsilon^{1/2} \frac{\lambda_{g_1}}{\lambda_0} \tag{4}$$

where

- λ_{g_ϵ} guide wavelength of the dielectric filled waveguide;
- λ_{g_1} guide wavelength of an air filled waveguide of identical cutoff frequency;
- ϵ dielectric constant, $\simeq 9$ for ruby.

At 22 GHz, a ruby-filled waveguide with cutoff frequency identical to WR-42 air filled guide (broad wall = 1.07 cm) has a slowing factor of 3.9. Thus from (2), an active ruby length of approximately 17.4 cm per stage is required (8.7-cm physical length) for 45 dB per stage of unbroadened gain. If the magnetic biasing field is tapered linearly by 132 G over approximately 8.7 cm of ruby length, the result should be 10 dB of gain per stage and a four-stage maser with 40 dB of electronic gain and 250 MHz of 3-dB bandwidth at 22 GHz. Similarly, 400 MHz of 3-dB bandwidth at 22 GHz is possible for a linear magnetic field taper of 190 G and 12.2 cm of physical ruby length.

Each of the parameters in (2) varies as the maser center frequency is tuned across the waveguide band. The active length N is directly proportional to frequency while the slowing factor S increases with decreasing frequency as the waveguide nears cutoff. These variations are shown in Fig. 4(a). The components of Q_m vary in different ways. The terms hf/kT and M^2 increase with frequency while the inversion ratio varies according to the expression [10]

$$I = 2\frac{f_{\text{pump}}}{f_{\text{signal}}} - 1. \tag{5}$$

When the inversion ratio is adjusted by a fixed offset to agree with the measured value of 1.8 at 22 GHz, the predicted variation of Q_m is as shown in Fig. 4(a). The net result is that the unbroadened gain is predicted to increase from 18 to 26 GHz as shown in Fig. 4(b).

The biasing magnetic field is tapered longitudinally by physically shaping the pole pieces of the magnet. As the center field value is varied in order to tune the maser, the spatial taper remains constant but the magnetic field taper, and thus Δf_0, increases with frequency as shown in Fig. 4(b).

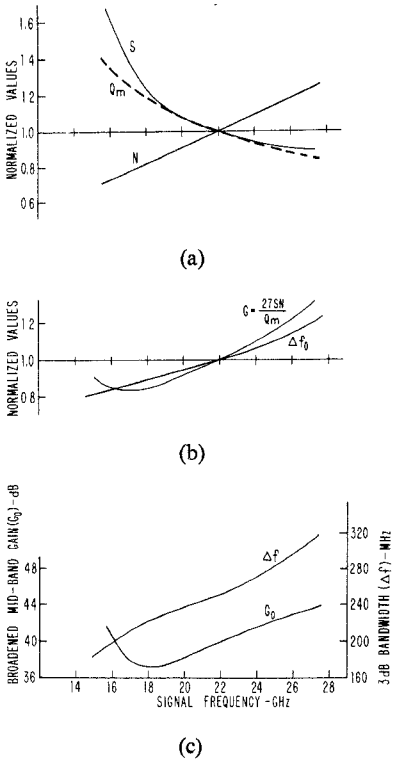

Fig. 4. Predicted variation with frequency of (a) slowing factor (S), active length (N), and magnetic $Q(Q_m)$; (b) unbroadened gain (G) and resonance separation (Δf_0); (c) mid-band gain (G_0) and 3-dB bandwidth (Δf).

When combined with (1) these variations result in the curves of Fig. 4(c) for broadened mid-band gain and 3-dB bandwidth. The 250-MHz bandwidth design is predicted to provide 37 to 43 dB of electronic gain and 220 to 300 MHz of 3-dB bandwidth as the center frequency is tuned from 18 to 26 GHz.

IV. Gain Ripple

Mismatch between the circulator junction and the ruby-filled waveguide will give rise to gain ripple which is represented by the expression

$$\text{ripple in dB} = 20 \log \left[\frac{\frac{1}{S_c} - R_m}{\frac{1}{S_c} + R_m} \cdot \frac{S_c + R_m}{S_c - R_m} \right] \tag{6}$$

where S_c is the equivalent VSWR of the circulator port and transition from ruby to air filled waveguide, and R_m is the real part of the maser normalized impedance ($R_m < 0$ for maser gain). R_m is related to the ideal net gain ($S_c = 1$) by

$$G_{\text{dB}} = 20 \log \left(\frac{1 - R_m}{1 + R_m} \right). \tag{7}$$

Fig. 5 is a plot of peak-to-peak gain ripple versus single-stage gain for various values of circulator junction match.

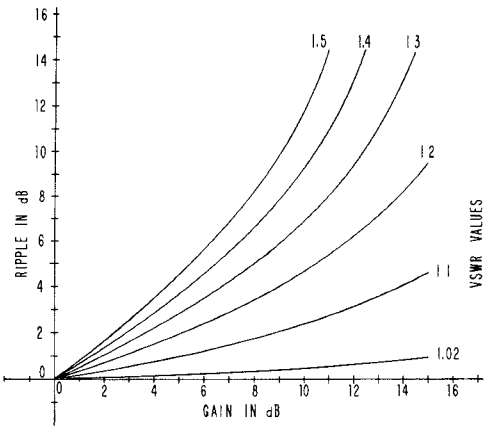

Fig. 5. Gain ripple dependence on gain and circulator junction VSWR for reflected-wave maser.

A typical circulator junction VSWR of 1.2:1 and stage gain of 9.5 dB leads to an expected gain ripple of 4.3 dB per stage. The ripple is repetitive in frequency at an interval determined by the time delay through each stage (approximately 170 MHz for this maser). The rubies were staggered in electrical length in order to cancel the expected ripple in pairs of stages.

Feedback around each amplifier stage can result in gain ripple which is also determined by (6). A typical circulator isolation of 20 dB and a load port return loss of 20 dB results in feedback which is 40 dB below the input. This can be equated to a VSWR at the circulator ruby port of 1.02, which with a stage gain of 9.5 dB results in a peak-to-peak ripple of 0.46 dB from each stage.

V. Noise Temperature

The maser noise temperature can be estimated from the following expression [11]:

$$T_e \simeq \frac{G-1}{G} T_0 \frac{\rho + \beta}{1 - \beta} \tag{8}$$

where

T_e effective single-stage maser noise temperature excluding input and output networks;
G single-stage electronic gain, dB;
T_0 cryogenic temperature of the maser material, K;
ρ inverse of the inversion ratio;
β $= \dfrac{\text{forward loss of maser structure in dB}}{\text{electronic gain in dB}}$.

For the maser under consideration at 22 GHz

$$G = 10 \text{ dB}$$
$$\rho = \frac{1}{1.8} = 0.56$$
$$\beta = \frac{0.5}{10} = 0.05$$
$$T_0 = 4.6 \text{ K}$$

and the single-stage effective noise temperature is 2.64 K.

Losses in the circulator junctions ahead of this (0.25 dB per pass) and the contribution of the second-stage increase the noise temperature at the circulator input to

$$T_{\text{maser}} \simeq (L_1 - 1)T_0 + L_1\left[T_{e_1} + \frac{(L_2 - 1)T_0 + L_2 T_{e_2}}{G_1}\right] = 3.96 \text{ K} \tag{9}$$

where L_1 and L_2 are the circulator junction losses preceding the first and second stages.

The contribution of the third and fourth maser stages adds an additional 0.13 K, and the zero-point energy [12] adds an additional 0.66 K ($\frac{1}{2}hf/k$). Thus the effective four-stage maser noise temperature referred to the input at the 4.6 K cryogenic station is 4.75 K. The very low structure loss permits the use of average values when calculating β. This approximation does not show the slight variation in noise temperature (± 0.5 K maximum) that exists across the instantaneous bandwidth due to the linear magnetic field taper.

VI. Maser Structure

The maser microwave structure is shown in Fig. 6. The ruby-filled waveguide is scaled by $\frac{1}{3}$ from air filled WR-42 waveguide. Its cross-sectional dimensions are 3.56×1.73 mm. A seven-step matching section combined with a gradually filling guide (ruby taper) provide the transition from the full width unfilled guide to the reduced width ruby-filled guide. (The height has been reduced to the proper dimensions at the circulator input.) This matching technique yields a VSWR of better than 1.2:1 across the waveguide band.

The rubies are tapered on only one side, leaving a flat (3.56-mm) surface with intimate contact to the flat copper divider plate along the entire length. Nylon pins with external springs are employed to apply pressure to the ruby to insure good thermal conduction to the copper. No other surface of the ruby needs to contact the copper waveguide. A gap of 0.01 mm between the ruby and the copper waveguide is used so that parts may be machined and assembled with ease, and problems caused by differential thermal expansion between the ruby and the copper waveguide are avoided. The gap across the 1.73-mm dimension affects the electric field, raising the cutoff frequency of the loaded waveguide ($\approx$14 GHz) about 3 percent. The gap does not degrade the match of the device in the 18–26.5-GHz range. Each ruby is approximately 15 cm in length, and the one-way transmission loss of the ruby-filled waveguide and matching section is estimated to be 0.25 dB at 4.6 K.

The rubies were oriented to within $\pm\frac{1}{8}°$ of the double-pump angle by observing coincidence of the 1–2 and 3–4 transitions. Each ruby was mounted in a shorted X-band waveguide and inserted between the pole pieces of a laboratory electromagnet. The spin resonance absorption

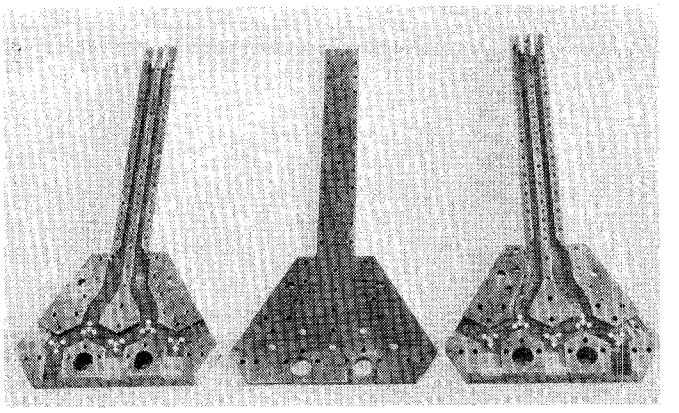

Fig. 6. The reflected-wave maser microwave structure.

of the 1–2 and 3–4 transitions were observed with an RF reflectometer as the magnetic field was swept and the field angle was adjusted for coincidence of the two transitions. The ruby was then turned end-for-end in the waveguide (using the same ruby face as an angular reference), and the procedure was repeated. The resultant angular difference in the two readings is twice the correction angle needed to be made to the ruby slab. In this manner, each ruby was properly oriented with respect to a reference face. The rubies were installed in the microwave structure with the reference face against the divider plate. This simple technique assures that the four rubies are mounted in the superconducting magnet to within $\pm\frac{1}{8}°$ of the double-pump angle.

VII. Circulator Block

The circulators are constructed in reduced height (1.73 mm by 10.67 mm) waveguide. A Y-junction below resonance design with nickel ferrite disks attached to the upper and lower waveguide broad walls is employed. A 0.254-mm gap between disks, and alumina matching blocks in the center of each waveguide arm, complete the design.[2] High-energy product rare-earth permanent magnets are used to bias the ferrite. The field is set about 1 kG below optimum at room temperature to account for the increase in magnet induction and ferrite saturation magnetization at 4.6 K. Single-junction isolation of 20 dB, insertion loss of 0.25 dB, and VSWR of 1.2:1 across the waveguide band are typical of 4.6 K performance.

The ten circulators are built in a three-piece copper block, with five circulators on each side sharing a common wall divider plate, as shown in Fig. 6. This construction permits a compact symmetrical design and allows magnetic biasing with only five sets of permanent magnets. Three section quarter-wave transformers are employed between full height and the reduced height waveguide at the input and output of each circulator block.

[2]Suggestions for this circulator design were provided by H. Saltzman of P and H Laboratories, Inc.

Terminated circulators used as isolators are employed between stages to attenuate signals traveling from output to input through the circulator block.

VIII. Superconducting Magnet

The superconducting magnet which biases the rubies is adjustable from 7.5 to 10 kG in order to tune the maser from 18 to 26.5 GHz. The magnet is a Cioffi-type [13] operating in the persistent mode and is similar to one developed for a K_u-band traveling-wave maser which operated at 7.5 kG [14]. The air gap was set at 1.54 cm at the widest (lowest field) point, and the pole pieces are 15.24 cm long. The pole pieces and return path are Hiperco 27 cobalt–iron machined and annealed to specification. This design contains the field with low leakage so that no detectable interaction with the circulator field occurs. The field was originally tapered by 190 G over a 12-cm length in order to achieve 400 MHz of bandwidth. Fringing at the ends of the pole pieces, however, resulted in a nonuniform field that reduced the useful length of the magnet to approximately 8 cm. The pole piece taper was relaxed, and iron compensation shims were added to achieve a field with a linear taper of 125 G over approximately 9 cm, which limits the bandwidth at 40-dB electronic gain to less than 250 MHz at 22 GHz.

IX. Microwave Pump

The microwave pump power is provided by a Siemens RWO 60 backward wave oscillator (BWO) selected for power output of at least 100 mW from 39 to 56 GHz. A single WR-19 waveguide carries the pump power to the base of the microwave structure where a power splitter and short length of dielectric-filled 1.73-mm square waveguide mates with the base of each ruby. The return loss at the pump input flange varies from 5 to 16 dB across the pump frequency range. A 20-kHz triangular wave ac voltage is combined with the BWO delay-line voltage in order to frequency modulate the pump frequency at up to 1000-MHz peak-to-peak deviation. Pump power is sufficient to nearly saturate the four stages at 240-MHz bandwidth (1-dB gain change for 1-dB pump power change).

X. Cryogenics

A closed-cycle helium refrigerator (CCR) is used to provide a 4.6 K operating environment for the maser, circulators, and superconducting magnet. Similar units have been used with many maser receiver systems throughout the NASA Deep Space Network [15].

XI. Maser Package

The entire assembly is housed in a vacuum dewar, and the OFHC copper input and output waveguides are thermally insulated with short sections of 0.254-mm wall, stainless-steel waveguide, copper plated on the inside to approximately three skin depths. The coin silver pump waveguide is similarly insulated. Commercial waveguide pressure windows are used on the input and output. A special window was fabricated for the pump waveguide vacuum seal. The package is shown in Fig. 7 with the vacuum dewar and heat shields removed to show the internal components. The input flange is at the top of the picture.

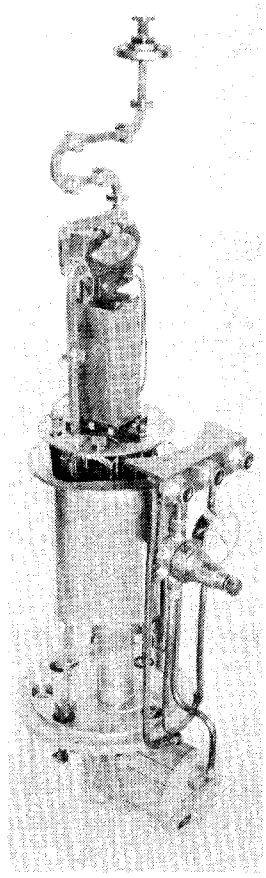

Fig. 7. The maser package with vacuum Dewar and heat shields removed.

XII. Performance

Initial tests of a single-stage maser which was designed as previously described yielded $5\frac{1}{2} \pm 1$ dB of net gain over 400 MHz centered at 19.45 GHz. However, fringing at the ends of the pole pieces reduced the useful length of the magnet to about 8 cm. Thus in the four-stage unit, the pole piece taper was relaxed to increase the gain at the expense of bandwidth. The best bandpass response is obtained near 22 GHz, and Fig. 8 shows the four-stage inversion ratio of 1.8, 3-dB bandwidth of 240 MHz, and 33 dB net gain achieved at this frequency. 1-dB gain compression occurs at an output signal level of approximately -35 dBm, which corresponds to approximately -68 dBm at the maser input.

The gain ripple becomes excessive for wide-band operation at the upper and lower quarters of the tuning range. The bandpass for tuning increments of 500 MHz are shown in Fig. 9, and are typical of the performance at intervening points. The bandwidth can be reduced electronically (reducing the pump frequency FM deviation) to

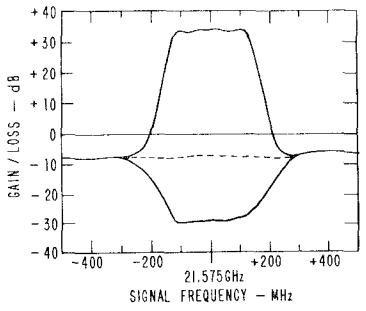

Fig. 8. Experimental gain and absorption near 22 GHz for the four-stage reflected-wave ruby maser.

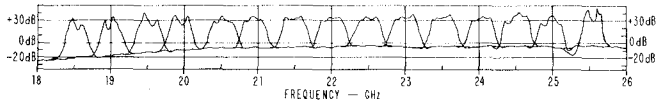

Fig. 9. Bandpass response of the four-stage reflected-wave maser at 500-MHz increments in the tuning range.

achieve a flattened response. 3-dB bandwidths in excess of 100 MHz can be achieved from 20.5 to 24 GHz and in excess of 30 MHz over the remainder of the band from 18.3 to 26.6 GHz.

Measured gain ripple indicates that the accumulated mismatch due to the circulator and ruby/vacuum-filled waveguide transition results in a VSWR that is probably no less than 1.4:1 near the band edges. It is further possible that the ripple cancellation via phasing of ruby pairs is not optimum. Subsequent units now under construction will permit measurement of the match and delay at this critical junction.

The noise temperature was measured as a complete amplifier system while looking vertically at the sky and included contributions from the cosmic background, atmospheric oxygen and water vapor, feed horn, and maser. The receiver following the maser contributed less than 2 K to the total system operating temperature, but the measurement technique eliminated inclusion of this quantity. Noise temperature values of 35 and 28 K were measured at 22.23 and 26.3 GHz, respectively. When allowances are made for the various contributions, the maser noise temperature at the room-temperature input flange is calculated to be 13 ± 2 K. An independent hot–cold load noise temperature measurement at 22.3 GHz indicated a maser noise temperature of 13.7 ± 4 K at this point.

XIII. Applications

A maser with this wide-bandwidth potential would find immediate application in continuum radio astronomy. More importantly, the wide-bandwidth capability can be used to good advantage for spectral line radio astronomy observations at millimeter frequencies where the structure in a spectra will often extend over 100 MHz [16]–[18]. By using the maser as an IF amplifier for cooled mixers or parametric downconverters [19], low noise temperature and wide bandwidth can be achieved at frequencies up to 230 GHz. At longer wavelengths, parametric upconverters in combination with K-band masers are planned to provide wide-bandwidth, low-noise operation at frequencies as low as L-band. The above techniques are presently under development for radio astronomy and spacecraft communications.

Preliminary results obtained with the K-band maser mounted on the NRAO 43-m antenna in a Cassegrain configuration show the following:

1) System noise temperatures (including atmospheric contributions) of 73 K at 22.23 GHz, 50 K below 20 GHz, and 60 K above 24 GHz during clear weather. The accumulated system noise temperature contributions from the feed horn, waveguide components, maser, and follow-up receiver are no greater than 30 K.

2) Total power variation equivalent to 0.15 K peak-to-peak for periods of tens of minutes during clear weather.

3) Gain stability (as measured with a calibration noise signal) of better than 4 percent (± 0.1 dB) for 5 h with the telescope tracking sources.

XIV. Conclusion

We have demonstrated the feasibility of a unique maser design for achieving wide instantaneous bandwidth and waveguide tuning range. Engineering problems which limit the bandwidth and result in excessive gain ripple have been outlined, and their resolution is now being pursued. Applications for this wide-band maser design are foreseen for both radio astronomy and planetary spacecraft communication.

References

[1] E. L. Kollberg, "A traveling wave maser system for radio astronomy," *Proc. IEEE*, vol. 61, pp. 1323–1329, Sept. 1973.

[2] M. S. Reid, R. C. Clauss, D. A. Bathker, and C. T. Stelzried, "Low-noise microwave receiving systems in a worldwide network of large antennas," *Proc. IEEE*, vol. 61, pp. 1330–1335, Sept. 1973.

[3] K. S. Yngvesson, A. C. Cheung, M. F. Chui, A. G. Cardiasmenos, S. Wang, and C. H. Townes, "K-band traveling-wave maser using ruby," *IEEE Trans. Microwave Theory Tech.*, vol MTT-24, pp. 711–717, Nov. 1976.

[4] E. L. Kollberg and P. T. Lewin, "Traveling-wave masers for radio astronomy in the frequency range 20-40 GHz," *IEEE Trans. Microwave Theory Tech.*, vol. MTT-24, pp. 718–725, Nov. 1976.

[5] S. Weinreb, M. Balister, S. Maas, and P. J. Napier, "Multiband low-noise receivers for a very large array," *IEEE Trans. Microwave Theory Tech.*, vol. MTT-25, pp. 243–248, Apr. 1977.

[6] F. S. Chen and W. J. Tabor, "Filling factor and isolator performance of the traveling-wave maser," *Bell Syst. Tech. J.*, pp. 1005–1033, May 1964.

[7] L. D. Flesner, S. Schultz, and R. Clauss, "Simple waveguide reflection maser with broad tunability," *Rev. Sci. Instrum.*, vol. 48, pp. 1104–1105, Aug. 1977.

[8] P. Warren, Union Carbide Corp., private communication.

[9] R. W. Berwin, "Paramagnetic energy levels of the ground state of Cr^{+3} in Al_2O_3(ruby)," Tech. Memo. 33-440, Jet Propulsion Lab., Jan. 15, 1970.

[10] A. E. Siegman, *Microwave Solid State Maser*. New York: McGraw-Hill, 1964, chs. 6 and 7.

[11] W. H. Higa, "Noise performance of traveling-wave masers," *IEEE Trans. Microwave Theory Tech.*, vol. MTT-12, p. 139, Jan. 1964.

[12] A. E. Siegman, "Zero-point energy as the source of amplifier noise," *Proc. IRE*, vol. 49, p. 633, 1961.

[13] P. P. Cioffi, "Approach to the ideal magnetic circuit concept

through superconductivity," *J. Appl. Phys.*, vol. 33, pp. 875–879, Mar. 1962.
[14] R. Berwin, E. Weibe, and P. Dachel, "Superconducting magnet for a Ku-band maser," in *Proc. 1972 Applied Superconductivity Conf.* (Annapolis, MD, May 1–3, 1972), pp. 266–269.
[15] W. H. Higa and E. Weibe, "A simplified approach to heat exchanger construction for cryogenic refrigerators," *Cryogenic Technol.*, vol. 3, pp. 47–48, 50–51, Mar./Apr. 1967.
[16] L. J. Rickard, P. Palmer, M. Morris, B. Zuckerman, and B. E. Turner, "Detection of extragalactic carbon monoxide at millimeter wavelengths," *Astrophys. J.*, vol. 199, pp. L75–L78, July 15, 1975.
[17] W. B. Burton, M. A. Gordon, T. M. Bania, and F. J. Lockman, "The overall distribution of carbon monoxide in the plane of the galaxy," *Astrophys. J.*, vol. 202, pp. 30–49, Nov. 15, 1975.
[18] B. Zuckerman, T. B. H. Kuiper, and E. N. R. Kuiper, "High-velocity gas in the Orion infrared nebula," *Astrophys. J.*, vol. 209, pp. L137–L142, Nov. 1, 1976.
[19] S. Weinreb, "Millimeter wave varactor down converters," presented at the Diode Mixers at Millimeter Wavelengths Workshop, Max-Planck-Institut für Radioastronomie, Bonn, West Germany, Apr. 1977.

Electrical Characterization of Transferred Electron Devices by a Novel Galvanomagnetic Technique

J. McBRETNEY AND M. J. HOWES

Abstract—**A novel technique is described that utilizes a galvanomagnetic phenomenon for the characterization of transferred electron devices. It is shown that this technique offers important advantages over present techniques based on the use of dummy packages and thus represents a useful analytical tool for the optimum design of transferred electron amplifier and oscillator circuits.**

I. Introduction

THE PERFORMANCE of transferred electron devices as microwave oscillators or amplifiers is critically dependent upon the microwave circuit in which they are embedded. Moreover, studies have indicated that the optimization of the microwave circuit (which includes the package) with regard to stability and noise in oscillators [1], [2] and stabilization and amplification characteristics in amplifiers [3], [4] requires a knowledge of the transferred electron device admittance.

The measurement of transferred electron device admittance is, however, complicated by the fact that the device is almost invariably encapsulated in a small package. Direct measurement, therefore, is impossible. Furthermore, at *X*-band frequencies and above, it would be futile to attempt the direct measurement of a "bare" chip since parasitics would seriously affect the measured admittance. An indirect method, therefore, must be adopted.

In this paper existing indirect methods are described briefly, and some of the disadvantages of their use are discussed. A new method based on galvanomagnetic effects is then described which circumvents these difficulties. It is shown that this technique enables the transfer matrix of a two-port network representing the package and mount to be evaluated and, hence, the device admittance found. Results for the admittance of the package and mount are compared with those based on the use of existing methods.

The method has been successfully applied to the characterization of various transferred electron devices having low contact and interfacial resistances.

II. Previous Methods of Device Characterization

Previous techniques for transferred electron device characterization have one feature in common. They require measurements to be made on particular configurations of dummy packages: that is, packages from which the active device has been removed and the internal geometry altered in some way. Two of these techniques will be considered here; the first is applicable to stable device characterization (amplifiers) while the second is applicable only to oscillating device characterization.

Manuscript received March 29, 1978; revised August 22, 1978.

J. McBretney is with the Ministry of Defence, Admiralty Surface Weapons Establishment, Portsdown Cosham, Portsmouth, England.
M. J. Howes is with the Department of Electrical Engineering, University of Leeds, Leeds, England.

0018-9480/79/0300-0256$00.75 ©1979 IEEE